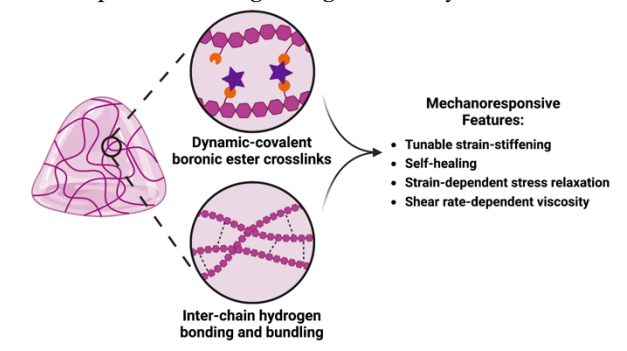
Strain-Stiffening Mechanoresponse in Dynamic-Covalent Cellulose Hydrogels

Rachel C. Ollier, Matthew J. Webber^{1,*}

- 1- University of Notre Dame, Department of Chemical & Biomolecular Engineering, Notre Dame, IN 46556 USA
- *- mwebber@nd.edu

ABSTRACT: Mechanical stimuli such as strain, force, and pressure are pervasive within and beyond the human body. Mechanoresponsive hydrogels have been engineered to undergo changes in their physicochemical or mechanical properties in response to such stimuli. Relevant responses can include strain-stiffening, self-healing, strain-dependent stress relaxation, and shear rate-dependent viscosity. These features are a direct result of dynamic bonds or non-covalent/physical interactions within such hydrogels. The contributions of various types of bonds and intermolecular interactions to these behaviors are important to more fully understand the resulting materials and engineer their mechanoresponsive features. Here, strain-stiffening in carboxymethylcellulose hydrogels crosslinked with pendant dynamic-covalent boronate esters using tannic acid is studied and modulated as a function of polymer concentration, temperature, and effective crosslink density. Furthermore, these materials are found to exhibit self-healing and strain-memory, as well as strain-dependent stress relaxation and shear rate-dependent changes in gel viscosity. These features

are attributed to the dynamic nature of the boronate ester crosslinks, inter-chain hydrogen bonding and bundling, or a combination of these two intermolecular interactions. This work provides insight into the interplay of such interactions in the context of mechanoresponsive behaviors, particularly informing the design of hydrogels with tunable strain-stiffening. The multi-responsive and tunable nature of this hydrogel system therefore presents a promising platform for a variety of applications.



KEYWORDS: stimuli-responsive materials; strain-stiffening; soft matter; bioinspired materials

1. INTRODUCTION

Mechanical stimuli and concomitant biological responses are pervasive in the living world. For example, matrix stiffness impacts stem cell differentiation, while other cells participate in long-range communication through changes to the stiffness of their extracellular matrix.¹⁻⁷ Variations in pressure exerted on blood vessel walls throughout the cardiac cycle result in changes in their diameters.^{8,9} Fibrin, a fibrillar protein that serves as a primary component of blood clots, stiffens in response to large strains or deformations, and in so doing prevents additional damage at wound sites.¹⁰ Inspired by these and other examples of mechanical stimuli, synthetic mechanoresponsive hydrogels have been designed for a wide variety of applications.

Hydrogels have high water content, porous structures, and are often biocompatible, which make these useful materials for many biologically relevant applications. 11-13 Mechanoresponsive hydrogels have been developed to undergo changes in their physical, chemical, and/or mechanical properties upon applied mechanical stimuli, including deformation, force, or pressure.14,15 The engineering of mechanically responsive features can empower a variety of applications. For example, hydrogels exhibiting shear-thinning and self-healing have been engineered and are widely utilized as injectable vehicles for drug delivery and 3D printing. 16,17 Shear-thinning and self-healing behaviors are typically a result of dynamic-covalent bonds or non-covalent interactions, such as hydrogen bonding, metal-ligand coordination, host-guest interactions, and hydrophobic

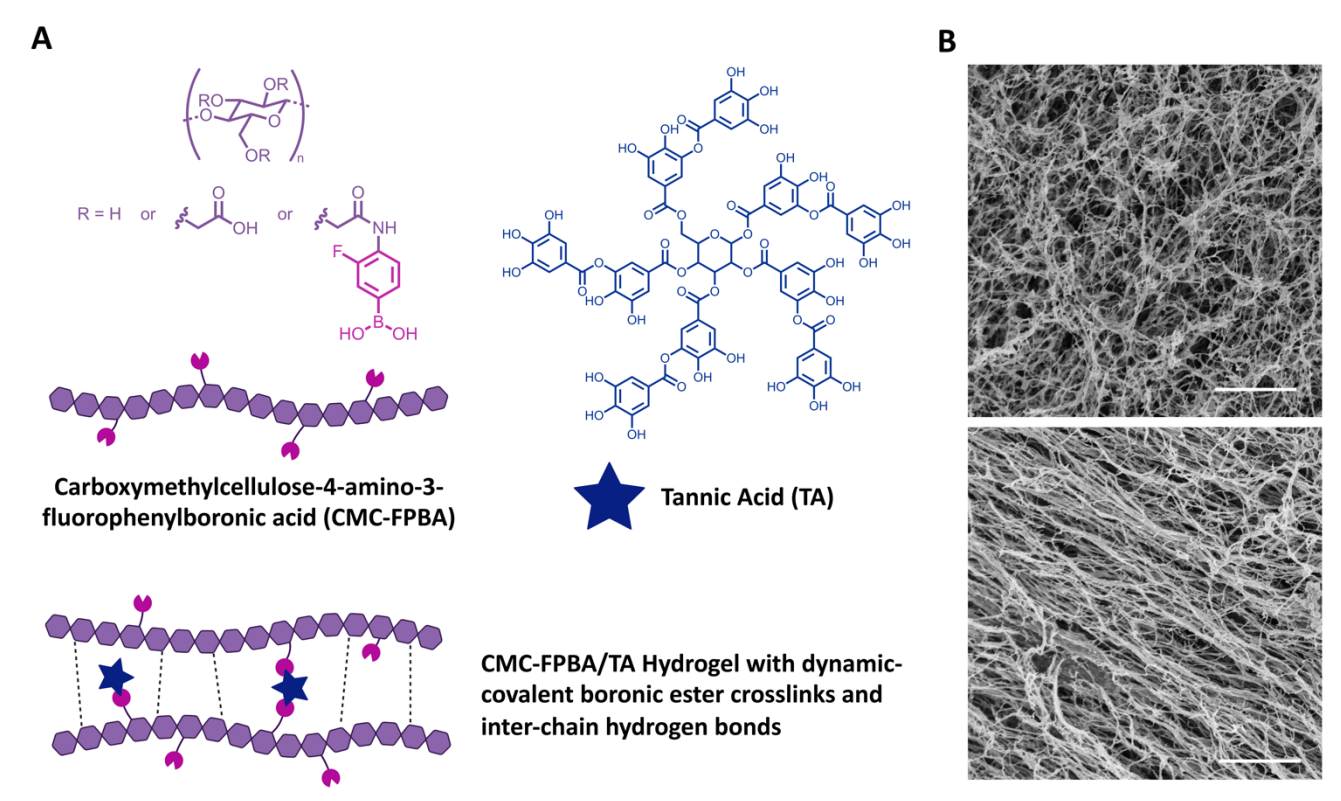


Figure 1: Hydrogels prepared from CMC-FPBA and TA. (**A**) Carboxymethylcellulose (CMC) modified with 4-amino-3-fluorophenylboronic acid (FPBA) was combined with tannic acid (TA), a naturally derived polyphenol, to prepare hydrogels with both dynamic-covalent boronic ester crosslinks and hydrogen bonds between CMC chains. (**B**) Representative SEM micrographs of a CMC-FPBA/TA gel (1% w/v, 20% CMC modification, diol:PBA ratio of 1:1, pH 7.4), showing regions of randomly oriented fibers (*top*) and hierarchical bundles of aligned fibers (*bottom*). Scale bars are 1 μm in both images.

interactions. 18-23 These relatively weak interactions are disrupted at high shear rates or high strains, but re-form upon cessation of the mechanical stimulus, allowing for recovery of the initial hydrogel mechanical properties. Strain sensors have been designed using strain-stiffening poly(acrylic acid)/poly(acrylamide) hydrogels, which display a deviation from linear viscoelasticity when their stiffness increases upon the application of high strain.^{24,25} Strain-stiffening oligo(ethylene)glycol polyisocyanopeptide hydrogels have also been used as synthetic extracellular matrices; the extent of their strain-stiffening response to deformations by encapsulated mesenchymal stem cells impacted the differentiation of these cells toward osteogenesis or adipogenesis.3 Additionally, strain-stiffening hydrogels have been engineered to exhibit muscle-like fatigue resistance.26-28

Strain-stiffening is a common feature of biopolymers and soft tissue, and is often attributed to physical interactions and entanglements of these relatively stiff polymer chains.²⁹⁻³¹ However, strain-stiffening has also been exhibited by an increasing number of synthetic hydrogels with various polymer backbones, some of which are flexible and do not participate in physical

entanglements, and many of which have dynamic or non-covalent crosslinking motifs.^{32–36}

It is apparent that the types of bonding and intermolecular interactions present in hydrogels dictate their mechanoresponses. The contributions of these different types of interactions is thus important in developing design principles for mechanoresponsive materials. Previously, we observed and characterized strain-stiffening in fully synthetic hydrogels prepared from 4-arm polyethylene glycol (PEG) crosslinked with dynamic-covalent boronate ester bonds.32 The near-ideal nature of these networks allowed for an exploration of the impact of polymer concentration, temperature, and pH, on strain-stiffening, almost entirely in isolation from chain interactions.37 However, these PEG gels lack structural similarity to gels prepared from strainstiffening biological polymers such as actin and collagen, which interact through hydrogen bonding. These physical bonds lead to further inter-chain interactions such as entanglement and bundling of polymer chains, adding structural complexity and giving rise to strainstiffening.^{29,31,38,39} Here, carboxymethylcellulose (CMC), a linear polymer with a similar propensity for physical hydrogen bonding interactions, is modified with phenylboronic acid (PBA) groups and subsequently crosslinked with tannic acid (TA), a naturally occurring small molecule polyphenol.40-42 A hydrogel network is formed from a combination of dynamic-covalent boronate ester bonds as well as hydrogen bonds and chain entanglements (Fig. 1A). The incorporation of hydrogen bonding motifs allows for closer replication of the hierarchical structures that govern many natural biological materials. SEM micrographs of a representative sample show a fibrillar network with regions of both randomly oriented and highly aligned chain bundles (Fig. 1B) Furthermore, the equilibrium-governed PBAdiol crosslinks in the material allow the mechanical properties of these gels to be controlled as a function of polymer concentration and crosslink density, as well as environmental conditions such as temperature and pH.37,43,44 Although these materials are crosslinked with the same dynamic-covalent boronate ester chemistry as the previously reported 4-arm PEG gels, their strainstiffening responses as a function of polymer concentration vary significantly, indicating intermolecular hydrogen bonding interactions and resulting chain entanglements contribute to both mechanical properties and mechanoresponsive nature of the hydrogels. In this work, strain-stiffening was characterized as a function of polymer concentration, temperature, degree of PBA modification on CMC, molar ratio of diol and PBA groups, and pH. In addition to strain-stiffening, these gels displayed self-healing, strainenhanced stress relaxation, and shear rate-dependent changes in viscosity. These various mechanoresponsive behaviors have been characterized and provide a deeper understanding of the contributions to mechanical properties attributable to dynamic-covalent bonding as well as hydrogen bonding and resulting physical chain entanglements.

2. MATERIALS & METHODS

2.1 Preparation of Hydrogels. Phenylboronic acid-modified carboxymethylcellulose (CMC) was prepared by activating CMC (90 kDa, 70% R-group carboxymethyl functionalization) with 4-(4,6-dimethoxy-1,3,5-triazin-2-yl)-4-methyl-morpholinium chloride (DMTMM), then adding 4-amino-3-fluorophenylboronic acid pinacol ester (AFPBA). By altering the ratios of DMTMM and AFPBA relative to the carboxyl groups on CMC, phenylboronic acid-modified carboxymethylcellulose (CMC-FPBA) was prepared with different degrees of modification. Full synthetic details may be found in the Online Supporting Information. To prepare hydrogels, FPBA-modified carboxymethyl cellulose (CMC-FPBA) was dissolved at 1.5% w/v in 1X phosphate buffered saline (PBS) at pH 7.4. Tannic acid (TA) was dissolved at 20 mg/mL in PBS. Due

to the acidity of TA, small volumes of 1M NaOH were used to adjust the pH of the TA solutions to 7.4, which was accounted for in the volumes used to prepare hydrogels. The CMC-FPBA and TA solutions were diluted with additional PBS and mixed to prepare CMChydrogels. Polymer FPBA/TA concentration, temperature, degree of polymer modification with PBA groups, ratio of diol groups relative to PBA groups (diol:PBA), and pH were individually probed for their impact on hydrogel mechanical properties and strainstiffening. In order to prepare hydrogels with 0.5, 1, 1.5, or 2% w/v polymer, the CMC-FPBA was dissolved at 2.5% w/v and diluted accordingly; TA solution was added in varying volumes to produce gels with diol:PBA of 1:1 for all samples. To test the impact of temperature, identical hydrogels were prepared at room temperature and then equilibrated to and tested at temperatures ranging from 5-35 °C on the rheometer. Hydrogels were prepared from CMC with degrees of modification of 10%, 20%, 25%, and 40% by dissolving each CMC sample separately; tannic acid was added in amounts that resulted in a diol:PBA ratio of 1:1 for each sample, while all other variables were held constant. Hydrogels with diol:PBA ratios of 3:1, 2:1, 1:1, 1:2, or 1:3 were prepared by varying the amount of TA added while keeping all other variables constant. Though the number of diol groups in commercially available tannic acid can vary, diol:PBA ratio was calculated using 10 diol groups per molecule, as seen in the formal structure (Fig. 1A). 45 Hydrogels were produced with pH ranging from 6-8 by preparing the CMC-FPBA and TA solutions with sodium phosphate buffer (50 mM, 100 mM NaCl) at the specified pH. The pH of the TA solutions were adjusted to the specified pH using small amounts of 1M NaOH or 1M HCl as needed. All samples were vortexed for 30 s to ensure complete mixing, and equilibrated at room temperature prior to testing on the rheometer.

2.2 Rheological Characterization. The mechanical properties of hydrogels were measured using a TA Instruments Discovery HR-2 Rheometer. A 20 mm 2° conical top plate with a solvent reservoir was used for all experiments, along with a sandblasted bottom geometry to reduce slippage of gels during testing. The reservoir on the top geometry was filled with water and a solvent trap placed around the rheometer stage to minimize sample drying. For experiments at varied temperatures, the gel was equilibrated at the testing temperature for 5 min. For all other experiments, gels were equilibrated for 60 s. Strain amplitude sweeps were performed on each gel at 10 rad/s from 0.1% to 500% strain. Frequency sweeps were conducted at 1% strain from 0.1 to 200 rad/s. In order to assess the reversibility and repeatability of the stiffening response, strain cycling analysis was performed at 10 rad/s. A low 1% strain was applied to gels for 100 s,

followed by a high strain of 25%, 50%, or 75% strain for 100 s. This was repeated for a total of three cycles. To understand the strain dependence of the stress relaxation behavior of these gels, constant strains of 25%, 50%, 65%, and 75% were applied, and the resulting modulus and stress were recorded. Shear rate sweeps were performed from 0.1 to $1000 \, \mathrm{s}^{-1}$ to characterize hydrogel viscosity.

2.3 Strain-Stiffening Analysis. Strain sweeps were performed on hydrogels with a range of polymer concentrations, temperatures, degrees of modification with PBA moieties, pH, and molar ratios of diol:PBA groups, prepared as described above. The strainstiffening responses of these gels were characterized as previously reported.³² The derivative of shear stress with respect to shear strain in a strain sweep is termed the differential modulus (K').31,38 When plotted as a function of shear stress on a log-log axes, K' shows two distinct regions: a low-stress linear viscoelastic region of nearly constant K', and a high-stress region showing strainstiffening as an exponential increase in K' as a function of shear stress. The intersection of these two linear regions is the critical stress (σ_c), the stress at which stiffening dominates the mechanical response of the network.³² The low-strain modulus (G₀) is the average value of the storage modulus (G') in the low-strain linear viscoelastic region. When K' is normalized against Go and plotted on log-log axes as a function of shear stress normalized by critical stress (σ/σ_c), similar low-stress plateau and highstress stiffening regions are present. The stiffening index (m) is determined to be the slope of this plot in the stiffening region, and is indicative of the magnitude of the strain-stiffening response of the network.31,33

2.4 Self-Healing Experiment. A visual, qualitative self-healing experiment was performed at room temperature by preparing two 1% w/v gels at pH 7.4, with 25% PBA modification of CMC and a diol:PBA ratio of 1:1. A small amount of either fluorescein isothiocyanate (FITC) or Rhodamine B was included in each gel. The gels were cut with a razor blade, and the cut sides of the two gels were placed together and allowed to heal for 1 min prior to physical manipulations and gross inspection of healing at the interface.

2.5 Scanning Electron Microscopy. Hydrogels were prepared for microscopy via serial dehydration with ethanol and critical point drying. After mounting, samples were sputter coated with iridium, and a small amount of silver paint was added to increase sample conductivity. The samples were imaged using a Magellan 400 field emission scanning electron microscope.

3. RESULTS & DISCUSSION

3.1 Hydrogel Network Design and Preparation.

Previously, we observed and characterized the strainstiffening behavior of hydrogels prepared from 4-arm PEG macromers crosslinked with dynamic-covalent boronate esters.³² Herein, the present studies further explore the impact of polymer backbone on strainstiffening in dynamic-covalent hydrogels, particularly in a non-ideal network where polymer chains interact with one another via hydrogen bonding. Accordingly, 4amino-3-fluoro-phenylboronic acid (FPBA) conjugated to carboxymethylcellulose (CMC) with DMTMM. Four different ratios of FPBA and DMTMM relative to carboxylic acid groups on CMC were reacted to obtain CMC-AFPBA with degrees of repeat unit functionalization with PBA of 10, 20, 25, and 40%, as quantified via ¹H NMR (Fig. S1).

Hydrogels were prepared by crosslinking CMC-FPBA with tannic acid (TA), a plant-derived small molecule polyphenol. The pK_a of this fluorine-substituted PBA is expected to be in the range of ~7.2-7.3,18,46 enabling PBAdiol bonding under conditions of 1X PBS at pH 7.4. Boronate esters exhibit pH-dependent formation and stability, and are more readily formed at or above the pK_a of the PBA.43,47,48 The FPBA motif thus allowed for preparation and characterization of these gels in a nearphysiological range of pH values. A reduced pK_a and corresponding decrease in pH required for gelation is also advantageous when considering TA is used here as a crosslinker. TA has multiple di- and tri-hydroxyphenyl groups; these groups form very strong complexes with PBAs, with K_{eq} of 830 M⁻¹ reported for PBA and catechol at pH 7.4.47 However, these functional groups are also prone to oxidation and polymerization, particularly in basic thereby inhibiting their crosslinking ability.42,49 Utilizing the FPBA motif to prepare the dynamic-covalent hydrogels described here allowed for sufficient crosslinking at pH values near neutral while minimizing the oxidation of TA.

Another challenge inherent to this hydrogel system was its formulation reproducibility. Because both crosslink density and propensity of TA to oxidize and polymerize are pH-dependent, slight variations in solution pH between samples or experimental days may result in variability in sample properties. Additionally, likely due to strong hydrogen bonding between polymer chains, many samples exhibited syneresis and excluded some volume of the buffer in which they were prepared, leading to variations in the effective polymer concentration when these materials were tested and also increasing the likelihood of slippage on the rheometer. Similar phase separation has previously been exhibited in a variety of gels,50-52 including galactomannan gels crosslinked by borate.53,54 In order to minimize these sources of experimental error, samples compared within

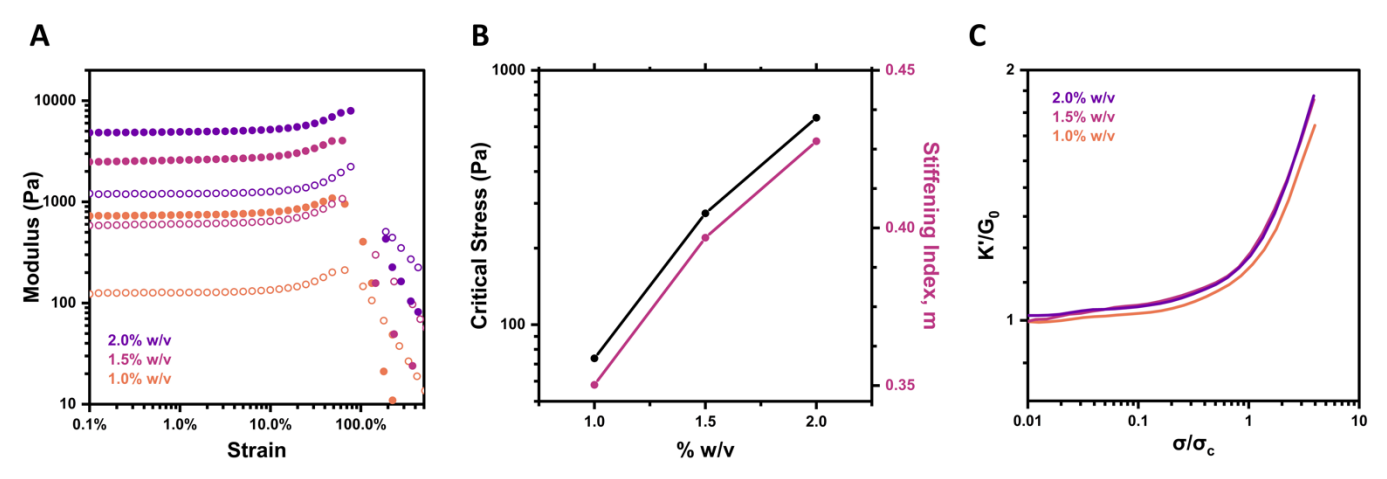


Figure 2: Concentration-dependent strain-stiffening behavior of CMC-FPBA/TA hydrogels (25 °C, 25% modification, diol:PBA ratio of 1:1, pH 7.4). (**A**) Storage modulus (G', *filled circles*) and loss modulus (G", *empty circles*) as a function of strain at 10 rad/s for gels prepared at 1-2% w/v. (**B**) Critical stress (σ_c , *left axis*) and stiffening index (m, *right axis*) as a function of polymer concentration. (**C**) Differential modulus (K') normalized by low strain modulus (G₀) as a function of stress (σ) normalized by critical stress (σ_c) for gels prepared at 1-2% w/v.

datasets were prepared and characterized on the same day whenever possible. Studies included multiple sample replicates and were repeated multiple times. The impact of polymer concentration, temperature, and effective crosslink density on strain-stiffening properties was also characterized by preparing or testing gel samples at a range of conditions.

3.2 Concentration-Dependent Strain-Stiffening. CMC-AFPBA/TA hydrogels were prepared at 1, 1.5, and 2% w/v with a fixed pH (7.4), diol:PBA ratio (1:1), CMC repeat unit functionalization (25%), and temperature (25 °C) in order to probe the impact of polymer concentration on the strain-stiffening response. Frequency sweeps and strain sweeps were performed on each gel. Frequency sweeps revealed slow crosslinking dynamics, with crossover frequencies of less than 0.1 rad/s for all concentrations, outside the observable experimental window (Fig. S2). Strain sweeps showed increasing gel stiffness with increasing concentration of CMC-AFPBA (*Fig. 2A*). For example, the G₀ of the 1% w/v gel was 747.9 Pa, while that of the 2% w/v gel was 4.9 kPa. This concentration dependence of gel stiffness was expected due to the increase in both dynamic-covalent crosslinks and polymer chain entanglements with increasing concentrations of CMC-AFPBA and TA. The overlap concentration of CMC is dependent on molecular weight degree of substitution (DS). The overlap concentration of 250,000 kDa CMC with DS of ~1.2 was found to be 0.07 mg/mL in water,55 indicating that CMC polymer chains are expected to physically interact with each other even at very low concentrations. Strain sweeps also displayed strain-stiffening behavior for all polymer concentrations tested, with the storage modulus increasing at elevated strains in each trace. The stiffening index (m), a measure of the degree of responsiveness of the material to stress that is generated as a result of

applied strain, was determined.^{31,33} The critical stress (σ_c), a measure of the stress at which the onset of stiffening is observed, was also determined. Critical stress has previously been shown to increase with G₀, the low-strain modulus.32,38 This present system performed similarly, as σ_c increased with G_0 as concentration was increased (*Fig.* **2B**). Critical stress increased from 73.8 Pa for the 1% w/v gel to 651.1 Pa for the 2% w/v gel, an increase of almost an order of magnitude. Though *m* reliably increased with increasing concentration, it spanned a relatively small range, increasing from 0.35 for a 1% w/v gel to only 0.43 for the gel prepared at 2% w/v. The small differences between the magnitudes of the stiffening responses for these gels may also be visualized in a plot of K'/G₀ as a function of σ/σ_c (*Fig. 2C*). The traces for gels prepared at all three polymer concentrations had very similar slopes and are nearly overlapping, indicating similar magnitudes of their respective responses to high shear strains. All three traces also had similar maximum values of K'/G₀, indicating that the maximum stiffening responses of these materials prepared at varying concentrations were comparable. The onset of the stiffening response, indicated by σ_c , was thus much more dramatically impacted than the magnitude of the response. Many recently explored strain-stiffening hydrogel systems have displayed decreases in m with increasing polymer concentration.31,33,56 However, small increases in m with increasing polymer concentration have also been observed. Carboxymethyl chitosan hydrogels crosslinked with telechelic dibenzaldehydeterminated PEG to form dynamic-covalent imine bonds exhibited similar small increases in m with increasing carboxymethyl chitosan concentrations.35 Similar to the CMC-FPBA/TA gels studied here, these gels contain both dynamic-covalent and hydrogen bonding motifs.

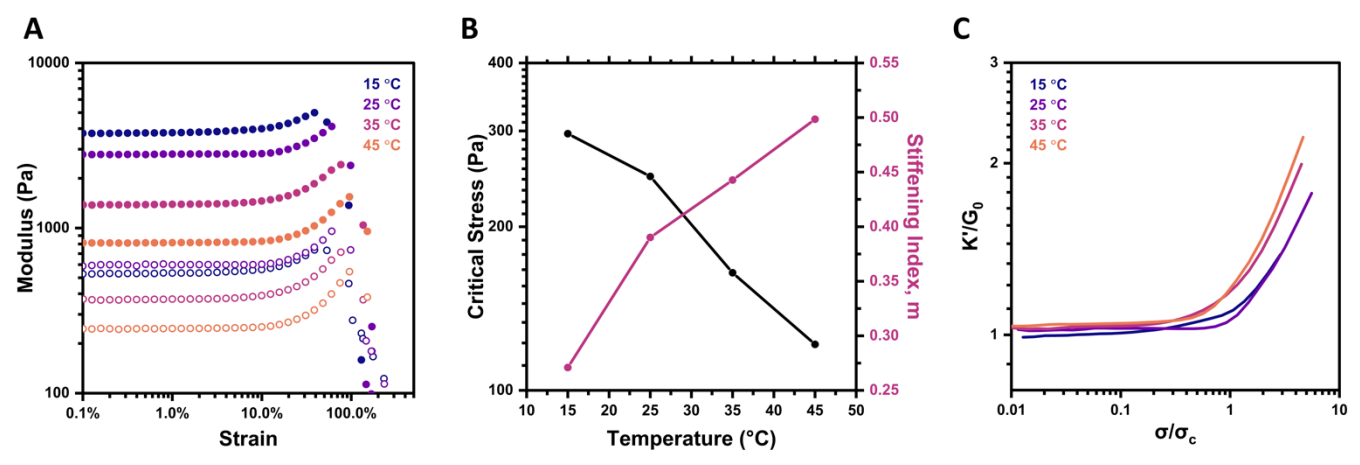


Figure 3: Temperature-dependent strain-stiffening behavior of CMC-FPBA/TA hydrogels (1% w/v, 25% modification, diol:PBA ratio of 1:1, pH 7.4). (**A**) Storage modulus (G', *filled circles*) and loss modulus (G'', *empty circles*) as a function of strain at 10 rad/s for gels at 15-45 °C. (**B**) Critical stress (σ_c , *left axis*) and stiffening index (m, *right axis*) of gels as a function of temperature. (**C**) Normalized differential modulus (K'/G₀) as a function of normalized stress (σ_c) for gels tested at 15-45 °C.

3.3 Temperature-Dependent Strain-Stiffening. equilibrium-governed dynamic bonds, the boronate ester crosslinks in this system are impacted by temperature. Increasing temperature serves to increase the prevalence of the entropically favored unbound state, increases the dynamicity of the crosslinks, and may also increase the flexibility of the cellulose chains.37,57,58 As a result, weaker gels were expected at elevated temperatures, relative to those tested at lower temperatures. Strain and frequency sweeps performed on 1% w/v gels (pH 7.4, diol:PBA 1:1, 25% repeat unit modification) at 15, 25, 35, and 45 °C followed this expected behavior (Fig. 3A, S3). Frequency sweeps again revealed slow crosslinking dynamics, with crossover frequencies below the experimental threshold of 0.1 rad/s, even at elevated temperatures. However, temperature-dependent gel stiffness was observed. The hydrogel analyzed at 15 °C had G₀ of 3.8 kPa, while the samples measured at 25, 35 and 45 °C had G₀ of 2.8 kPa, 1.6 kPa, and 817.3 Pa, respectively. The values for σ_c also decreased with increasing temperature, from 296.5 Pa for the gel tested at 15 °C to 121.5 Pa for the gel tested at 45 °C (Fig. 3B). Additionally, as testing temperature was increased and resulted in weaker gels, the magnitude of the strain-stiffening response of these materials increased, visible in traces of K'/G₀ as a function of σ/σ_c for different testing temperatures (Fig. 3C), the slopes of which were quantified in plots of *m* as a function of temperature (*Fig.* 3B). The hydrogel tested at 15 °C stiffened from a G_0 of 3.8 kPa to a maximum G' of 5.0 kPa, an increase of 32%, and had an m of 0.27. The hydrogel tested at 45 °C stiffened from Go of 817.3 Pa to a maximum G' of 1.5 kPa, an increase of 89%, and had an m of 0.50. The inverse relationship between gel stiffness and m realized by varying temperature contrasted with the concentrationdependent strain-stiffening behavior of this system, in

which gels with higher polymer concentrations were both stiffer and stiffened to a greater extent.

3.4 Strain-Stiffening as a Function of Effective Crosslink Density. Effective network crosslink density can be tuned in multiple ways in this hydrogel system; degree of polymer modification with PBA functional groups, ratio of diol:PBA groups incorporated in the gel, and pH all impact crosslink density in this system without varying polymer concentration. In this way, the contributions of dynamic-covalent crosslinking can be studied. However, the CMC backbone polymer has its own intermolecular interactions from hydrogen bonding and chain bundling and entanglements, and these may be further impacted by pendant crosslink density. As such, the contributions of each of these modes of interactions between polymer chains are unlikely to be fully isolated. For example, it is possible that an increase in crosslink density will constrain chain orientation in a manner that decreases the likelihood of interchain bundling. In order to further study the relationship between network crosslink density and strain-stiffening response, the degree of modification, diol:PBA molar ratio, or pH of CMC-AFPBA/TA gels were varied while keeping all other variables constant.

Increasing the degree of repeat unit functionalization served to increase the quantity of crosslinking points along the polymer chains, and likewise involved proportionally increasing the amount of TA crosslinker in the network in order to maintain a constant diol:PBA ratio. For all degrees of polymer modification, hydrogels were prepared at 1% w/v, pH 7.4, diol:PBA 1:1, and tested at 25 °C. The higher degrees of modification and resulting increases in crosslink density produced stiffer networks, as seen in frequency and strain sweeps of hydrogels

prepared with CMC in which 10, 20, 25 or 40% of repeat units were modified with PBA groups (*Figs. S4, 4A*). The frequency sweep revealed concentration-dependent dynamics, as the gels prepared with CMC with degrees

of modification of 20%, 25%, and 40% had crossover frequencies below 0.1 rad/s, while the gel prepared with 10% PBA-functionalized CMC had a crossover frequency of 5.5 rad/s (*Fig. S4*). Upon increasing from 10% to 20%

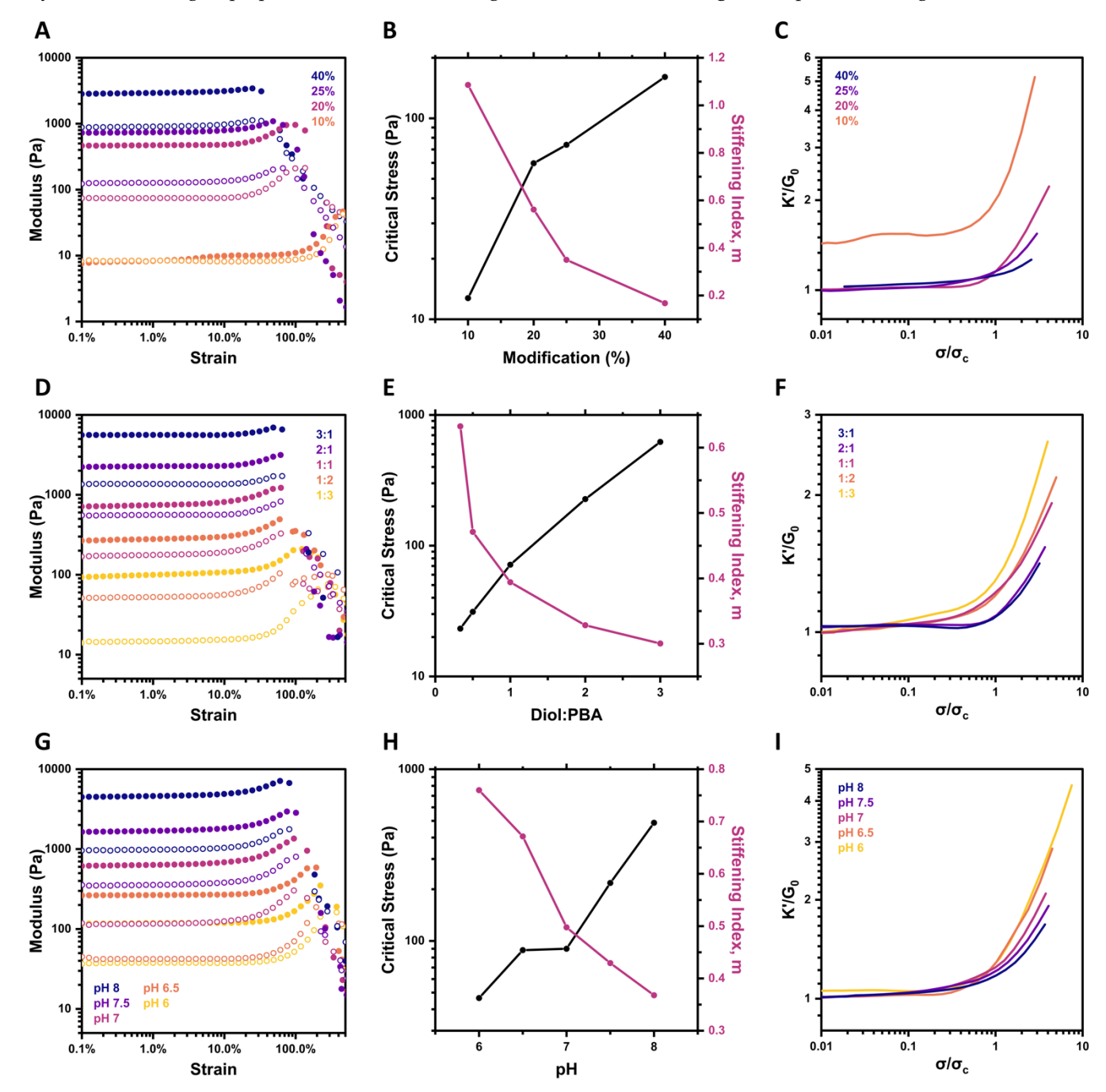


Figure 4: Strain-stiffening behavior of CMC-FPBA/TA hydrogels as a function of effective crosslink density (1% w/v, 25 °C). (A) Storage modulus (G', *filled circles*) and loss modulus (G", *empty circles*) as a function of strain at 10 rad/s for gels prepared from CMC with repeat unit functionalization of 10-40% with FPBA groups (diol:PBA 1:1, pH 7.4). (B) Critical stress (σ_c , *left axis*) and stiffening index (m, *right axis*) of gels as a function of degree of CMC modification. (C) Normalized differential modulus (K'/G₀) as a function of normalized stress (σ /c) for gels prepared with 10-40% modified CMC. (D) Storage modulus (G', *filled circles*) and loss modulus (G", *empty circles*) as a function of strain at 10 rad/s for gels prepared with diol:PBA molar ratios from 1:3-3:1 (25% modification, pH 7.4). (E) Critical stress (σ /c, *left axis*) and stiffening index (m, *right axis*) of gels as a function of the molar ratio of diol:PBA functional groups. (F) Normalized differential modulus (K'/G₀) as a function of normalized stress (σ / σ /c) for gels prepared with diol:PBA molar ratios from 1:3-3:1. (G) Storage modulus (G', *filled circles*) and loss modulus (G", *empty circles*) as a function of strain at 10 rad/s for gels prepared at pH 6-8 (25% modification, diol:PBA 1:1). (H) Critical stress (σ /c, *left axis*) and stiffening index (m, *right axis*) of gels as a function of pH. (I) Normalized differential modulus (K'/G₀) as a function of normalized stress (σ / σ /c) for gels prepared at pH 6-8.

modification, Go increased from 8.5 Pa to 470.7 Pa. When modification was increased further, to 25% and 40%, Go increased to 746.1 Pa and 2.9 kPa, respectively (Fig. 4A). Values of σ_c also increased with increasing degree of modification, from 12.7 Pa for the gel prepared with 10% PBA-modified CMC to 59.8, 73.8, and 160.6 Pa for gels prepared with 20%, 25%, and 40% PBA-modified CMC, respectively (Fig. 4B). The m was determined from a plot of K'/G₀ as a function σ/σ_c for each degree of modification (Fig. 4C). As the degree of modification and gel stiffness increased, m decreased (Fig. 4B). The hydrogel prepared with 10% PBA-functionalized CMC and the lowest crosslink density had an m of 1.1, while the hydrogels prepared with degrees of crosslinking of 20%, 25%, and 40% PBA modification had values of m of 0.56, 0.35, and 0.17, respectively. Overall, very broad ranges of mechanical properties and strain-responsiveness were accessed by varying the quantity of crosslinkable functional groups present in the network.

Diol functional groups were included in the network via incorporation of the TA crosslinker. PBA functional groups are covalently bound to and presented on the CMC backbone. The ratio of these two functional groups determines the extent of crosslinking possible in the network, given that other systemic variables are held constant. In this study, the amount of TA was varied to produce gels with diol:PBA molar ratios of 3:1, 2:1, 1:1, 1:2, and 1:3, while the gels were otherwise prepared identically (1% w/v, pH 7, 25% repeat unit functionalization, 25 °C). As expected, this impacted the mechanical properties of the resulting gels, as observed in strain and frequency sweeps (Figs. 4D, S5). Gels prepared with diol:PBA ratios less than 1:1 had relatively fewer diol groups available to form crosslinks and thus were weaker, with Go of 99.9 Pa and 280.5 Pa for hydrogels prepared with diol:PBA ratios of 1:3 and 1:2, respectively. As diol:PBA ratio was increased to 1:1, 2:1, and 3:1, Go increased to 746.1 Pa, 2.2 kPa, and 5.6 kPa, respectively. All crossover frequencies remained below 0.1 rad/s (Fig. S5). Values of σ_c increased with increasing diol:PBA molar ratio, from 23.2 Pa for a 1:3 diol:PBA ratio to 622.1 Pa for a gel with a 3:1 diol:PBA molar ratio (Fig. 4E). In an ideal network hydrogel, a molar ratio of 1:1 for crosslinking functional groups results in an optimally crosslinked network, with minimal dangling ends, and continued increase in the concentration of crosslinker reduces the effective crosslinking and ideal-like nature of the network and results in a weaker gel.59 Here however, as evidenced by the continued increase in stiffness as the ratio of diol:PBA groups is increased above 1:1, this present hydrogel system is non-ideal. Based on the proximity of the many catechol groups on one TA molecule, there are steric limitations that prevent all of these groups from binding at one time. As a result,

increasing the concentration of tannic acid and diol functional groups increased the crosslink density in the network. Similar to varying the degree of modification of CMC chains with PBA groups, increasing the ratio of diol groups relative to PBA groups produced stiffer gels which stiffened to a lesser degree. This is visible qualitatively from traces of K'/G_0 as a function of σ/σ_c for samples prepared with a range of diol:PBA ratios (Fig. 4F) as well as quantitatively from plots of m as a function of the diol:PBA ratio. As the molar ratio of diol groups to PBA groups was increased from 1:3 to 3:1, m decreased from 0.63 to 0.3, and the maximum value of K'/G₀ decreased from 2.6 to 1.4. Although a smaller range of *m* resulted from varying diol:PBA than from the degree of functionalization of the CMC chains with PBA groups, similar trends were observed. Conditions promoting a higher crosslink density resulted in stiffer gels with a lower capacity for strain-stiffening.

The pH of the gel relative to the pK_a of the PBA used, ~7.2-7.3 for FPBA,18,46 determines the fraction of PBA motifs that are able to form stable crosslinks with diols. Increasing pH increases the fraction of PBAs in their negatively charged tetrahedral boronate state, which form more stable, hydrolysis-resistant bonds with diols than their uncharged boronic acid counterparts. 43,44 This results in an increase to Keg for PBA binding to diols as pH is increased.⁴⁷ However, increasing pH also increases the propensity of the catechol groups in TA to oxidize to quinones, which can further react and polymerize. 42,49,60,61 Despite this complication of using TA as a crosslinker, increasing pH generally increased gel stiffness, as seen in strain sweeps of hydrogels prepared at pH 6-8 (1% w/v, diol:PBA 1:1, 25% repeat unit functionalization, 25 °C) (Fig. 4G). The gel prepared at pH 6 had G₀ of 118.3 Pa. The G₀ increased to 265.9 Pa, 633.1 Pa, 1.7 kPa, and 4.6 kPa for hydrogels prepared at pH 6.5, 7, 7.5, and 8, respectively. These gels also displayed pH-dependent strainresponsiveness. The onset of stiffening, quantified by σ_c , increased with increasing pH, similar to G₀. The gel prepared at pH 6 had σ_c values of 46.5 Pa, while those prepared at pH 8 had a σ_c of 536.4 Pa, more than an order of magnitude higher (Fig. 4H). As seen when varying the degree of polymer modification or the ratio of diol and PBA functional groups in these hydrogels, stiffer gels had a less acute response to high strain. The values of mdecreased from 0.76 for the gel prepared at pH 6 to 0.37 for the stiffest gel, prepared at pH 8 (Fig. 4H). This behavior can also be observed from plots of K'/G₀ against σ/σ_c for each pH (Fig. 4I). The slope in the stiffening regime and the maximum value of K'/G0 decreased with increasing pH. Additionally, frequency sweeps of these gels revealed pH-dependent dynamics (Fig. S6). The gel prepared at pH 6 had a crossover frequency of 0.42 rad/s,

while the crossover frequency of gels prepared at pH 6.5-8 were all less than 0.1 rad/s.

As exhibited by studies varying the degree of modification of polymer chains with PBA groups, the molar ratio of diol:PBA, and the pH at which the gel is prepared, a general trend emerges wherein increasing crosslink density decreased the strain-responsive nature of these materials. This is in contrast to the concentrationdependent strain-stiffening behavior of these materials. Increasing the concentration of CMC-FPBA (and proportionally TA, to maintain a constant diol:PBA ratio of 1:1), and thereby simultaneously increasing both polymer chain density and crosslink density in the network, increased the extent of strain-responsiveness displayed by the network. Based on this difference, it is proposed that the primary driving force of the strainstiffening response is the non-covalent interactions between CMC-FPBA chains, such as hydrogen bonding, chain entanglement, and the formation of chain bundles. However, these non-covalent interactions alone are not sufficient to create a material that is capable of stiffening in response to strain. A 1% w/v solution of 25% modified CMC-FPBA with no tannic acid was prepared at pH 7.4, and a strain sweep and frequency sweep were performed on this material at 25 °C (Fig. S7). The strain sweep revealed characteristics of a very weak gel, with Go of 0.94 Pa and G'>G'' until a failure strain of ~5.7%. No stiffening was observed on this strain sweep. The primary response of this material to strain was to flow rather than stiffen. It is thus inferred that some number of dynamic-covalent crosslinks are required for this material to form a gel capable of stiffening in response to strain. Therefore, there is likely to be some critical crosslink density required for this behavior. However, increasing the density of these dynamic-covalent crosslinks beyond the critical density likely inhibits the ability of CMC chains to form structures such as bundles that would promote strain-stiffening. Increased crosslink density results in a more rigid and organized network structure that, under strain, minimizes chain alignment in the direction of strain and resulting bundle formation.33,35,62 The high affinity of PBA groups for the dihydroxyphenol or catechol groups in tannic acid is expected to contribute to this behavior.⁴⁷ This affinity will promote crosslinking, likely at the cost of inter-chain interactions. A high fraction of PBA groups will be in the bound state at any given time. Because the hydrodynamic diameter of tannic acid, ~1 nm for a solution of tannic acid prepared at pH 7.4,63 is larger than the typical length of hydrogen bond interactions, ~2-3 nm,64,65 an increase in crosslink density in the network may force CMC chains into conformations that inhibit chain entanglement and bundling. Additionally, due to their high affinity, these PBA-dihydroxyphenol bonds are not very dynamic relative to other, lower affinity PBA-diol bonds (*Fig. S2-S6*).^{37,59} Their less frequent reorganization thus minimizes time in the unbound state and the opportunity for chain entanglement. The decreased strain-stiffening response observed in this system with increasing crosslink density is thus attributed to a network structure that minimizes the impact of inter-chain hydrogen bonding and resists strain-induced chain alignment and bundling.

3.5 Response to Cyclic Strain. Gels were also subjected to cycles of low and high strain in order to explore the reversibility and repeatability of the strain-stiffening response of these materials. In this experiment, three 1% w/v hydrogels were prepared at pH 7.4 with diol:PBA 1:1, 25% repeat unit modified CMC-FPBA, and tested at 25 °C and 10 rad/s. Each gel was subjected to 1% strain for 100 s followed by 25%, 50%, or 75% strain for 100 s, and this process was repeated for a total of 3 cycles of low and high strain. The storage modulus through the course of these cycles is normalized by the average value of the storage modulus in the initial low-strain period (G'/G0) and plotted against time (Fig. 5). It was anticipated that 1% strain would not result in significant stiffening of these gels, and a plateau would be observed throughout the low-strain period. When applied strain was increased, the gels were expected to stiffen notably, as seen in strain sweeps of this material (Figs. 2A, 3A, 4A, 4D). In these gels, however, a small amount of stiffening was observed throughout even the initial period during which 1% strain is applied. The storage moduli of the three samples increased an average of 9.7 Pa throughout the first 100 s. The responses of the three samples deviated in the following high-strain period when varying strains were

The first gel tested had an average storage modulus of 421.4 Pa throughout the initial 1% strain period. When a 25% strain was applied, the gel instantaneously stiffened, with G' increasing to 473.4 Pa and G'/Go increasing to 1.12. The gel continued to gradually stiffen under 25% strain, with G'/G_0 increasing to a maximum of 1.14 by the end of the first high-strain period. When the applied strain was decreased back to 1% following the first period of high strain, the gel softened rapidly. G' instantaneously decreased to 443.4 Pa, corresponding to G'/G₀ of 1.05. Within 1 s, the gel further softened to G' of 435.4 Pa. The stiffness of the gel then remained approximately constant through this low-strain period, with an average G' of 434.4 Pa and average G'/G_0 of 1.03. The remainder of this trace follows a similar pattern: the gel instantaneously stiffened when the applied strain was increased to 25% and instantaneously softened when the strain was decreased to 1%. During these periods of low and high strains, the stiffness of the gel increased minimally, remaining approximately constant. During the second high-strain period, G' increased slightly from 484.3 Pa to 486.9 Pa. During the third period of 25% strain, G' increased just 0.8 Pa, from 491.2 Pa to 492.0 Pa. In the intermediate third low-strain period, the gel maintained an average stiffness of 442.9 Pa, corresponding to an average G'/G_0 of 1.05.

A second gel was tested, and 1% and 50% strains were alternatingly applied for 100 s intervals. Based on strain sweeps of these materials (Figs. 2A, 3A, 4A, 4D), 50% strain is approximately the strain at which the peak G' was observed for hydrogels of this composition. Following a period during which 1% strain was applied and the average G' was 539.9 Pa, the gel instantaneously stiffened under 50% strain. G'/Go increased from 1.01 at the end of the low-strain period to 1.35 upon 50% strain. As opposed to the small increase in stiffness observed throughout the application of 25% strain, the stiffness of this gel gradually decreased throughout the high-strain period. A maximum G' of 730.9 Pa was observed after 3.9 s under 50% strain, corresponding to G'/G₀ of 1.35. The gel then relaxed throughout the high-strain period, reaching G' of 666.4 Pa and G'/G₀ of 1.23 at 100 s. Upon a decrease in the applied strain back to 1%, the stiffness of the gel decreased, with G' of 562.6 Pa and G'/G0 of 1.04 at the beginning of the second low-strain period. Throughout this period, the stiffness of the gel gradually increased, reaching a maximum G' of 576.0 Pa and G'/Go of 1.07 by the end of the period. When the applied strain was increased to 50% for the second time, the gel instantaneously reached a maximum G'/Go of 1.34, corresponding to G' of 726.0 Pa. The gel then proceeded to steadily soften, more rapidly and to a greater extent than in the first high-strain period, reaching a minimum G' of 630.1 Pa and G'/G_0 of 1.17. Once again, upon decreasing strain to 1%, G'/Go decreased, reaching a minimum of 1.07 and then increasing slightly to 1.09 by the end of the final low-strain period. The final highstrain period followed a similar pattern as the first two, with gel stiffness instantaneously increasing to G'/Go of 1.32 upon the application of 50% strain. The gel stiffness then rapidly decreased, with G'/G₀ reaching 1.20 within 10.5 seconds at 50% strain and 1.15 at 33.1 seconds. The gel also weakened to a greater degree than in either of the first two periods of 50% strain. The gel reached a minimum G' of 567.9 Pa and G'/G0 of 1.05 by the end of the final high-strain period, less stiff than it was during the previous low-strain period. Based on the trend of the three cycles of 1% and 50% strain applied in this experiment, it is expected that further high-strain periods would result in instantaneous peaks in stiffness followed by larger and increasingly rapid decreases in stiffness.

A third gel was subjected to alternating 100 s periods of 1% and 75% strain. From strain sweeps on these gels

(Figs. 2A, 3A, 4A, 4D), 75% strain is higher than the strain at which the peak G' value is observed, but it is less than the failure strain at which G'' > G'. Similar to the first two gels described, the third gel stiffened slightly during the initial low-strain period, with G' increasing from 548.7 Pa at the beginning of the period to 563.7 Pa at the end. When the applied strain was increased to 75%, G' instantaneously increased to 882.9 Pa, corresponding to G'/G_0 of 1.58. The stiffness of the gel proceeded to rapidly decrease throughout the remainder of the first high-strain period, reaching G' of 274.2 Pa and G'/G₀ of 0.49 by the end of the period. In the following low-strain period, the gel rapidly recovered and maintained approximately constant stiffness, with average values for G' and G'/G0 of 557.4 and 1.00, respectively, for the second low-strain period. At the beginning of the second high-strain period, the rheometer overshot the increase in strain (Fig. S8), initially applying a 93.8% strain, corresponding to a G' of 394.8 Pa and G'/G_0 of 0.71. As the strain decreased to 75% over the following ~5 s, the gel stiffness also decreased, reaching G' of 234.2 Pa and G'/Go of 0.42. The gel continued to weaken throughout the remainder of the high-strain period, decreasing to G' of 145.3 and G'/G₀ of 0.26. When the applied strain was decreased to 1%, the gel once again rapidly recovered. The gel stiffness was approximately constant throughout this third low-strain period, with G' and G'/G₀ averaging 563.5 Pa and 1.01, respectively. The rheometer again overshot the increase in strain at the beginning of the third high-strain period, initially applying a strain of 102.9% (Fig. S8). Under this strain, the stiffness of the gel decreased to G' of 214.8 Pa and G'/G_0 of 0.38. The gel stiffness continued to decrease as the strain was decreased to 75% over the following ~5 s, reaching G' of 118.7 Pa and G'/G₀ of 0.21. Throughout the remainder of the high-strain period, the gel weakened further, reaching a minimum G' of 92.4 Pa and G'/G₀ of 0.17. Though the stiffness of the gel did not change as much during the third period as in the first or second, it did reach the lowest G' and G'/G₀ values of the entire experiment. The gel also displayed the most rapid decrease in stiffness during this period. It is interesting to note that the high-strain portions of the trace for the gel, during which time 75% strain was applied, appear nearly continuous. Despite being interrupted by periods of 1% strain and the subsequent sharp drop-offs upon the application of high strain, the periods during which 75% strain was applied to this gel appear as if they could have been immediately consecutive to one another. A parallel behavior was displayed by the gel to which 50% strain was applied. This gel responded to 50% strain by first increasing in stiffness, then weakening more rapidly and to a greater extent each time the applied strain was increased to 50%. Both of these behaviors are indicative of some form of gel memory, in which the gel carries the history of past applied strains. It is possible that this is a result of the strain-induced alignment of polymer chains, or the formation of other semi-permanent structures within the gel that do not rapidly dissipate upon a decrease in applied strain.^{62,66,67}

3.6 Self-Healing Behavior. The dynamic nature of the crosslinks between the catechol groups of TA and the pendant PBA groups on CMC allow the material to rapidly self-heal. This behavior was exhibited in the strain-cycling experiments previously described (Fig. 5A). The application of 75% strain resulted in the rupture of some fraction of PBA-diol crosslinks and a notable decrease in G'. When the applied strain was decreased, these bonds reformed and G' increased, returning back to the baseline G'/G₀ of 1. To demonstrate this behavior on a macroscopic scale, two 1% w/v gels were prepared at room temperature and pH 7.4, with 25% degree of modification of CMC and a diol:PBA ratio of 1:1. Prior to the addition of the TA solution, a small amount of fluorescein isothiocyanate or Rhodamine B was added to each vial to enhance visibility of the two gels. Once crosslinked and mixed, the gels were cut (Fig. 5B) and placed together. After one minute, the two gels had healed sufficiently to remain attached when physically manipulated and be self-supporting when suspended (Fig. 5C).

3.7 Strain-Dependent Stress Relaxation. Viscoelastic polymeric materials exhibit stress relaxation, a decrease in stress over time upon the application of a constant strain, a behavior typically attributed to the rearrangement of polymer chains.⁶⁸ The hydrogels reported here have an additional time-dependent element in their dynamic-covalent crosslinking. The dynamic nature and constant exchange of these bonds also allows for relaxation of stress.^{59,68} The hydrogen bonds underlying bundling of CMC chains are also dynamic, with bond lifetimes on the order of 1 picosecond in water,⁶⁹ allowing them to be pulled apart and reformed.

The oscillatory strain-cycling previously described revealed a strain-dependent rate of decrease of the storage modulus (*Fig. 5A*). The application of 25% strain (oscillatory, 10 rad/s) did not result in a decrease in storage modulus, but when 50% strain was applied, the modulus decreased over time. The modulus decreased rapidly the first time 75% strain was applied, and instantaneously the second and third times. These decreases in G' are expected to be due to the strain-dependent rupture of PBA–diol crosslinks over time. This phenomenon is also expected to impact stress relaxation. A strain-enhanced rate of crosslink rupture is likely to correspond to a strain-enhanced rate of stress relaxation. S6.59 In fact, strain-dependent stress relaxation has previously been reported for biopolymer gels.⁷⁰ The

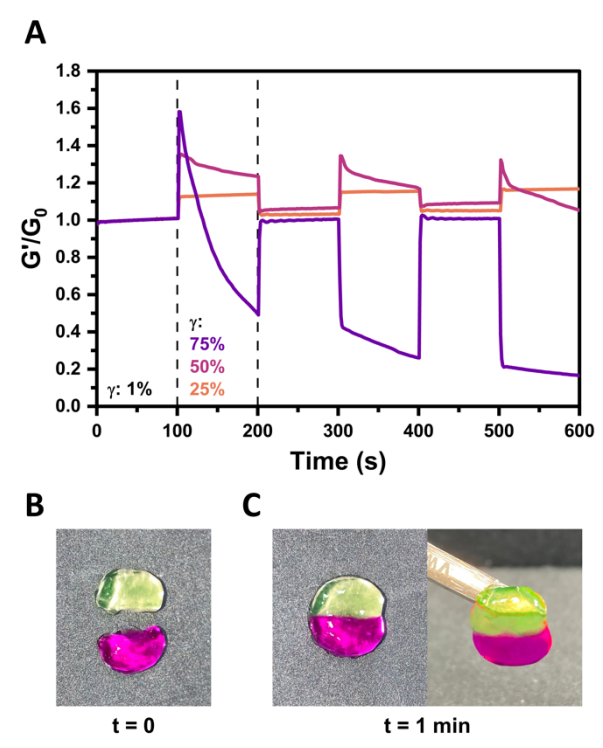


Figure 5: Strain-cycling and self-healing behavior of CMC-FPBA/TA hydrogels (1% w/v, 25 °C, 25% modification, diol:PBA ratio of 1:1, pH 7.4). (**A**) Storage modulus (G') normalized by initial low-strain modulus (G₀) as a function of time over three continuous cycles of low strain (1%) and high strain (25, 50, or 75%) at 10 rad/s. (**B**) CMC-FPBA/TA hydrogels colored with a small amount of fluorescein isothiocyanate (*green*) or Rhodamine B (*pink*). (**C**) The two CMC-FPBA/TA hydrogel gels immediately after being placed together (*left*) and suspended after being placed together for 1 min (*right*).

application of increased strains resulted in an increase in stiffness of fibrin and type-1 collagen gels, two of the multiple fibrillar proteins that display strain-stiffening. Increased strains also resulted in increased rates of stress relaxation for these gels. When the fibrin and collagen were crosslinked with factor XIII and glutaraldehyde, respectively, the resulting gels also exhibited strain-dependent stress relaxation, although to a lesser extent. It is hypothesized that strain-enhanced stress relaxation is due to force-dependent crosslink disassociation, with higher strains and thus higher forces increasing the probability of bond dissociation.^{56,70}

In order to characterize the impact of the magnitude of applied strain on the stress relaxation response of CMC-FPBA/TA gels, a 1% w/v hydrogel was prepared at pH 7.4 with 25% modification and a diol:PBA ratio of 1:1. At 25 °C, a 25% strain was applied to the hydrogel, and the stress relaxation behavior was monitored. The hydrogel was then allowed to recover for 5 min. Strains of 50%, 65%, and 75% were then applied, with a 5 min recovery between each stress relaxation test. Shear stress (σ) was plotted as a function of time for each applied strain (Fig. 6A). Under all applied strains, the gel displayed relatively fast stress relaxation, with σ initially decreasing rapidly, then continuing to decrease more gradually. The strainstiffening response of these materials was also evident from this plot, with higher applied strains resulting in increased stresses. The initial shear stress (σ_0), calculated as an average of the first 10 points from each trace, increased from 247.7 Pa for 25% strain to 766.0, 1496.3, and 2366.2 Pa for 50%, 65%, and 75% strain, respectively. The shear stress was normalized by the initial shear stress (σ/σ_0) and plotted as a function of time (*Fig. 6B*). A strain dependence in the rate of stress relaxation was visible from this normalized data. When the gel was strained to 25%, it had the slowest rate of decrease of σ/σ_0 . Increased strains resulted in increased rates of stress relaxation, with the 75% strain revealing the most rapid stress relaxation. The relaxation time (τ_R) was calculated as the time for σ/σ_0 to decrease below 1/e and was used to quantify the rate of stress relaxation. When τ_R was plotted against strain (Fig. 6C), it decreased from 6.2 s for 25% strain to 3.7 s for 50% strain, 2.1 s for 65% strain, and 1.3 s for 75% strain. This data revealed a linear relationship between τ_R and applied strain, with $R^2 = 0.999$.

These stress relaxation tests at four different strains were all run on the same gel sample to avoid the sampleto-sample variation inherent to this material. In order to verify that the application of prior strains was not enhancing the rate of stress relaxation, a second control experiment was performed in which 50% strain was applied to one gel 5 times, with a 5 min recovery between each run. The gel was prepared at 1% w/v, pH 7.4, with 25% modification and diol:PBA of 1:1, and was tested at 25 °C. Stress was plotted as a function of time for each run (*Fig. S9-A*). The initial stress (σ_0) was calculated for each run in the same manner as described above, and increased from 344.0 Pa for the first run to 825.3 Pa for the 5th run. However, when the stress for each run was normalized by the corresponding initial stress (Fig. S9-B), the traces of σ/σ_0 as a function of time largely overlapped. The first run relaxed slightly faster than subsequent runs, which was reflected in a plot of τ_R as a function of the run number (Fig. S9-C), showing TR increased slightly from a value of 1.32 s for the first run to 1.84 s for the second run, then plateaued, remaining nearly constant for runs 2-5. As a result, it is expected that the repeated application of strain did not contribute to the increased rate of stress relaxation upon the application of increasing strains. Instead, it is proposed that elevated strains, under which larger forces are applied to network crosslinks, increase the rate of bond dissociation.71 As the network relaxation time is a function of the rate of crosslink dissociation,

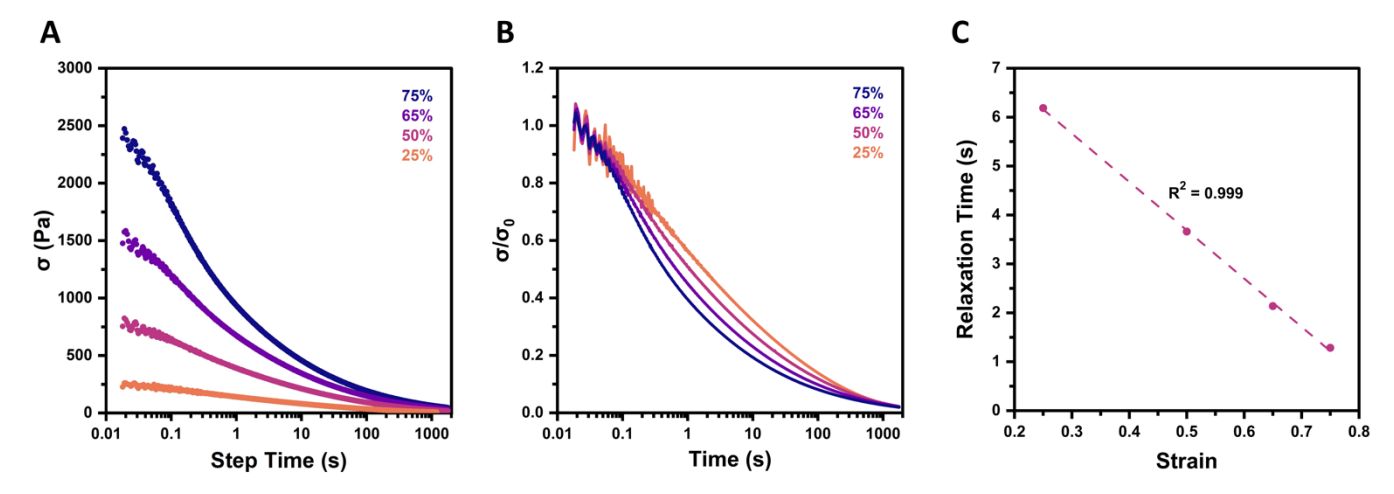


Figure 6: Strain-dependent stress relaxation of CMC-FPBA/TA hydrogels (1% w/v, 25 °C, 25% modification, diol:PBA ratio of 1:1, pH 7.4). (**A**) Shear stress (σ) as a function of time for stress relaxation experiments in which 25, 50, 65, and 75% strain were sequentially applied to a sample, with a 5 min recovery period between each strain. (**B**) Shear stress normalized by initial shear stress (σ / σ ₀) as a function of time for shear strains of 25-75%. (**C**) Relaxation time, determined as the time required for σ / σ ₀ to reach 1/e, as a function of shear strain. Dashed line represents a linear fit with the coefficient of determination (R²) shown.

elevated strains allow for more rapid stress relaxation. 56.59 Additionally, as the network is strained and crosslinks are disrupted, polymer chains will reorganize, reducing the frequency of rebinding between newly dissociated PBA and diol motifs.. As such, it is possible that the network will experience a strain-dependent reduction in crosslink association rate. Both of these contributions would suggest a decrease in the effective equilibrium constant of the network.

3.8 Hydrogel Viscosity as a Function of Shear Rate. Dynamic-covalent hydrogels have gained interest in applications such as drug delivery and 3D printing, in part due to their expected extrudability or injectability. This property is a function of the dynamic nature of the crosslinks that give rise to hydrogel formation and govern mechanical properties. The application of a high shear rate to a dynamic-covalent hydrogel, such as during extrusion from a syringe, results in crosslink rupture, decreasing the material viscosity and allowing it to flow more easily. Following injection, the crosslinks are able to reform and restore the original mechanical properties of the gel. It is typically observed that such materials will display shear-thinning immediately following a plateau, or "zero-shear" viscosity, period. However, following the low shear rate plateau, the CMC-AFPBA/TA hydrogels displayed a region of shear-thickening, characterized by an increase in viscosity with increasing shear rate (Fig. 7A). At yet higher shear rates, the hydrogel displays the dramatic decrease in viscosity with increasing shear rate that is characteristic of shear-thinning materials.

A shear rate sweep was performed at 25 °C on a 1% w/v hydrogel prepared at pH 7.4 with a diol:PBA ratio of 1:1, using 25% repeat unit modified CMC-FPBA. The shear rate was increased from 0.001 s⁻¹ to 1000 s⁻¹, and the viscosity of the hydrogel was recorded. Upon plotting viscosity as a function of shear rate (Fig. 7A), a region of nearly constant viscosity was observed at low shear rates. This region was followed by an increase in viscosity with increasing shear rate. This increase was made more visible when viscosity was normalized by the initial low shear rate viscosity, or "zero-shear" viscosity, (η/η_0) and plotted as a function of shear rate (Fig. 7B). The maximum viscosity, 4703.0 Pa·s, occurred at a shear rate of 0.10 s-1. This viscosity was more than three times the initial viscosity, 1518.2 Pa·s, with a peak η/η_0 of 3.1. This maximum was followed by a rapid decrease in viscosity, with η/η_0 decreasing to 0.29 at a shear rate of 0.51 s⁻¹, and 0.11 at 1.0 s⁻¹.

Shear-thickening has recently been observed in a limited number of hydrogel systems. In gels prepared from poly(alkylene oxide)-grafted hyaluronic acid or CMC, shear-thickening was attributed to a shear-induced increase in inter-chain crosslinking.⁷² Intermediate shear

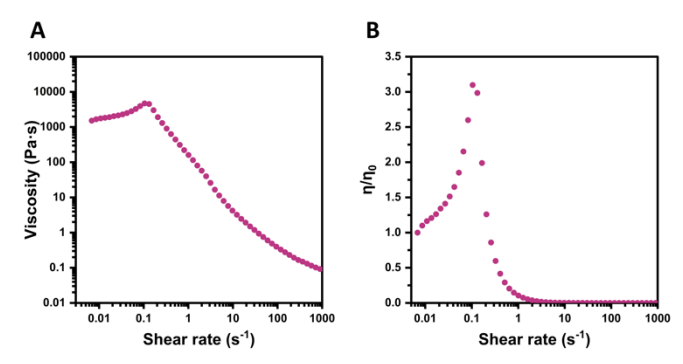


Figure 7: Steady shear rheometry performed on a CMC-FPBA/TA hydrogel (1% w/v, 25 °C, 25% modification, diol:PBA ratio of 1:1, pH 7.4). (**A**) Shear rate sweep characterizing hydrogel viscosity as a function of shear rate. (**B**) Hydrogel viscosity normalized by initial zero-shear viscosity (η/η_0) as a function of shear rate.

rates were expected to result in the extension of polymer chains in the direction of flow. Chain extension exposes regions of these polymers that were previously coiled and participating in intra-chain interactions, allowing such regions to participate instead in inter-chain interactions. Shear-thickening behavior has also been observed in hydrogels prepared from 4-arm PEG macromers with dynamic-covalent Thia-Michael crosslinks.73 These hydrogels displayed a low-shear plateau followed by a region of shear-thickening, which was primarily attributed to chain stretching. Following the shearthickening regime, these gels displayed flow instability, which limited the range of shear rates experimentally available. This flow instability was characterized by an abrupt decrease in shear stress and a discontinuity in the plot of shear stress as a function of shear rate. By comparison, in the shear rate sweep performed on the CMC-FPBA/TA hydrogel, the shear stress rapidly but continuously decreased with increasing shear rate beyond the shear-thickening regime. As a result of this smooth and continuous curve, it is thought that this shear-thickening response is a true material property. The CMC-FPBA/TA gel prepared here displayed shearthickening up to a shear rate of 0.10 s-1, followed by shearthinning for the remainder of the shear rate sweep.

The reversibility of this shear-dependent viscosity was characterized by performing two consecutive shear rate sweeps. Shear rate was increased from 0.001 to 1000 s⁻¹ in the first sweep, then immediately decreased from 1000 to 0.001 s⁻¹ in the second sweep. The viscosity traces from these two shear rate sweeps largely overlap at shear rates above 0.1 s⁻¹ (*Fig. S10*). During this period, dynamic-covalent crosslinks and hydrogen bonds are being ruptured as shear rate is increased and are being reformed as shear rate is decreased. Hysteresis was observed at shear rates below 0.1 s⁻¹. This low shear rate regime revealed shear-thickening when shear rate was

increased from 0.001 to 0.1 s⁻¹. When shear rate was instead decreased from 0.1 to 0.001 s⁻¹, the viscosity continued to increase. This result alludes to a shear-driven increase in inter-chain interactions at low shear rates. Upon increasing shear rate in this regime, chains are extended and aligned, resulting in additional inter-chain hydrogen bonding. However, when shear rate is decreased in this regime, these bonds will remain intact and viscosity will continue to increase. In contrast, if chain stretching were primarily responsible for shear-thickening in these gels, no hysteresis would be expected, and reversibility of thickening in the low-shear regime would be observed.⁷³

Shear rate sweeps were also performed at temperatures ranging from 15-45 °C (Fig. S11-A). Viscosity was normalized by the low shear rate viscosity (η/η_0) and plotted as a function of shear rate (*Fig. S11-B*). It is apparent from these plots that increasing temperature decreased gel viscosity and increased the shear rates at which the onset of shear-thickening and the onset of shear-thinning occurred. Decreased viscosity at elevated temperatures is due to decreased intermolecular interactions, both dynamic-covalent bonds and physical hydrogen bonds. While the maximum normalized viscosity increased when temperature was increased from 15 °C to 25 and 35 °C, it decreased when the temperature was further increased to 45 °C (Fig. S11-C). As there is no definitive dependence of the magnitude of shear-thickening on temperature in CMC-FPBA/TA gels, this behavior is not likely to be driven by dynamiccovalent crosslinking, the equilibrium of which is significantly affected by temperature. Instead, it is attributed to shear-induced chain extension and a conversion of intra-chain hydrogen bonding to interchain hydrogen bonding. However, high shear rates rupture crosslinks and hydrogen bonds and result in shear-thinning and a decrease in material viscosity. In the CMC-AFPBA gels characterized here, shear-thinning begins at 0.1 s-1, resulting in injectable materials at shear rates relevant for applications such as syringe injection and 3D printing, ranging from approximately 103-105 s-1 74,75

3.9 Interplay of Dynamic-Covalent Crosslinking and Physical Bonding for Mechanoresponsive Properties. The mechanical properties of the CMC-FPBA/TA gels described here are the result of two primary interactions: (1) dynamic-covalent bonds between the pendant PBA groups on the CMC chains and the di- and trihydroxyphenyl groups on TA, and (2) hydrogen bonding between CMC chains and the ensuing chain bundling and entanglement. The strain-stiffening, self-healing, strain-dependent stress relaxation, and shear rate-dependent viscosity that this material displayed are a result of these

interactions. It is valuable to understand the interplay of these interactions as it relates to the resulting mechanoresponsive behavior.

From a strain sweep at 25 °C of a 1% w/v solution of CMC-AFPBA prepared at pH 7.4 with 25% modification and no TA crosslinker (Fig. S7-A), it is apparent that gel stiffness is primarily dependent on the density of boronic ester crosslinks in the network. This material had a G' less than 1 Pa, with Go of 0.94 Pa. The incorporation of dynamic-covalent crosslinks through the addition of TA transformed the properties of this material. Even gels prepared with relatively low effective crosslink densities had increased stiffness and displayed strain-stiffening. (Fig. 4 A,D,G). The weakest gel prepared with TA in this study had a 10% modification and Go of 8.5 Pa. Two other relatively weak gels, those prepared with a diol:PBA ratio of 1:3 or at pH 6, had G₀ of 99.9 Pa and 118.3, respectively. All of the hydrogels prepared with TA in this work also displayed strain-stiffening. The onset and magnitude of the strain-stiffening response varied with polymer concentration, temperature, and effective crosslink density. Accordingly, when σ_c , indicative of the onset of strain-stiffening, was plotted as a function of Go for gels prepared at all conditions and for all variables explored here, σ_c increased linearly with G_0 with an R^2 of 0.90 (*Fig.* S12). When polymer concentration was varied, TA concentration was varied proportionally to maintain a constant diol:PBA ratio while keeping all other variables constant. As a result, both the concentration of dynamiccovalent crosslinks and hydrogen bonds are expected to increase. When CMC concentration was varied, the value of m, indicative of the magnitude of strain-stiffening, increased with increasing polymer concentration. In contrast, when polymer concentration was held constant and effective crosslink density was varied, m decreased as effective crosslink density increased. This result, consistent among studies that varied the degree of modification, diol:PBA ratio, and pH, leads to a conclusion that while dynamic-covalent crosslinks are required to form a material capable of responding to strain, strain-stiffening is primarily driven by the physical interactions between polymer chains in this hydrogel material. When the concentration of dynamic-covalent crosslinks is minimized, inter-chain hydrogen bonding and bundling is expected to dominate gel behavior. Hydrogen bonding and physical inter-chain interactions are also expected to play a more dominant role at elevated temperatures. Under these conditions, dynamic-covalent crosslinks are more dynamic and the entropically favored unbound state is more prevalent, yet physical interactions are affected to a lesser extent.37,57,76 It is expected that the application of high strains results in an extension of polymer chains in the direction of strain, allowing for increased hydrogen bonding.62,72,77 Chain alignment also likely increases the propensity for chain bundling.⁶⁷ Both of these factors would result in an increase in gel stiffness and a resistance to strain. This proposed mechanism of strain-stiffening is consistent with that of many biopolymer gels.31,70,78 Increasing the density of boronate ester crosslinks results in a more rigid network, in which polymer chains are less able to align in the direction of strain and create structures that resist continued strain. Similarly, it is anticipated that the shear-thickening behavior exhibited by these gels is a result of shearinduced chain alignment and an increase in hydrogen bonding.67,72,73,77 This results in an increase in stiffness prior to shear-thinning. Accordingly, it is expected that shear-thinning results primarily from the rupture of boronate ester crosslinks at high shear rates. Such shear rates may also disrupt hydrogen bonding and bundling between CMC chains, further decreasing viscosity. Selfhealing is a common feature of hydrogels crosslinked with dynamic bonds. The dynamic nature of both the boronate ester crosslinks and inter-chain hydrogen bonds in this network likely contribute to the rapid self-healing exhibited by the CMC-FPBA/TA gels studied here. Dynamic-covalent bonds and hydrogen bonds also exhibit strain-dependent rates of bond rupture.56,59,70,71 This translates to strain-dependent stress relaxation, as bond rupture serves as a mechanism to dissipate stress in the hydrogel network. It is therefore anticipated that this phenomenon is a cooperative result of the straindependent rupture of both the boronate ester crosslinks and inter-chain hydrogen bonds present in the CMC-FPBA/TA gel networks.

The CMC-FPBA/TA gels characterized in this work exhibited many forms of mechanoresponsive behavior as a result of the two distinct types of intermolecular interactions between polymer chains: dynamic-covalent boronate ester crosslinks and hydrogen bonds. This work therefore offers further understanding of the contributions of these interactions, both individually and cooperatively, towards mechanoresponsive behavior of hydrogels. This knowledge will aid in the design and optimization of further mechanoresponsive materials.

4. CONCLUSIONS

Inspired by the variety of mechanical stimuli and mechanoresponses found in natural biological materials, synthetic hydrogels have been engineered to exhibit comparable responses to mechanical stimuli. This work reports a hydrogel system in which CMC is modified with a PBA motif and crosslinked with TA, a small molecule polyphenol. The resulting hydrogels displayed strain-stiffening that was tuned as a function of polymer concentration, temperature, and effective crosslink

density. The extent of strain-stiffening in these hydrogels increased with increasing polymer concentration, but decreased with increasing concentration of boronate ester crosslinks, indicating that strain-stiffening was driven primarily by hydrogen bonding between polymer chains. The material also exhibited self-healing as a result of the dynamic-covalent boronate ester crosslinks, and straindependent stress relaxation. Shear rate-dependent changes in viscosity were also observed, as the material initially shear-thickened, then shear-thinned. This hydrogel platform provided insight into the interplay between dynamic-covalent crosslinks and hydrogen bonding as they impact mechanical properties and mechanoresponsive behavior. This understanding is valuable for designing future bioinspired materials. The multi-mechanoresponsive nature and hierarchical structure of this system also makes it a promising soft material for a variety of biologically inspired and biologically relevant applications.

ASSOCIATED CONTENT

Supporting Information

The Supporting Information is available free of charge on the ACS Publications website:

Detailed Synthetic Methods; Supplemental Data (.PDF)

AUTHOR INFORMATION

Corresponding Author

* mwebber@nd.edu

Notes

The authors declare no competing financial interests.

ACKNOWLEDGMENT

MJW gratefully acknowledges funding support for this work from the National Science Foundation (BMAT, 1944875), the American Diabetes Association Pathway Award (1-19-ACE-31), and the Juvenile Diabetes Research Foundation (5-CDA-2020-947-A-N). TOC graphic and Figure 1 created using Biorender.com.

REFERENCES

- (1) Sopher, R. S.; Tokash, H.; Natan, S.; Sharabi, M.; Shelah, O.; Tchaicheeyan, O.; Lesman, A. Nonlinear Elasticity of the ECM Fibers Facilitates Efficient Intercellular Communication. *Biophys. J.* **2018**, *115* (7), 1357–1370.
- (2) Guvendiren, M.; Burdick, J. A. Stiffening Hydrogels to Probe Short- and Long-Term Cellular Responses to Dynamic Mechanics. *Nat. Commun.* 2012, 3, 792.
- (3) Das, R. K.; Gocheva, V.; Hammink, R.; Zouani, O. F.; Rowan, A. E. Stress-Stiffening-Mediated Stem-Cell Commitment Switch in

- Soft Responsive Hydrogels. Nat. Mater. 2016, 15 (3), 318–325.
- (4) Liu, K.; Mihaila, S. M.; Rowan, A.; Oosterwijk, E.; Kouwer, P. H. J. Synthetic Extracellular Matrices with Nonlinear Elasticity Regulate Cellular Organization. *Biomacromolecules* 2019, 20 (2), 826–834.
- (5) Hall, M. S.; Alisafaei, F.; Ban, E.; Feng, X.; Hui, C.-Y.; Shenoy, V. B.; Wu, M. Fibrous Nonlinear Elasticity Enables Positive Mechanical Feedback between Cells and ECMs. *Proc. Natl. Acad. Sci. U. S. A.* 2016, 113 (49), 14043–14048.
- (6) Kloxin, A. M.; Kloxin, C. J.; Bowman, C. N.; Anseth, K. S. Mechanical Properties of Cellularly Responsive Hydrogels and Their Experimental Determination. *Adv. Mater.* 2010, 22 (31), 3484–3494.
- (7) Schultz, K. M.; Kyburz, K. A.; Anseth, K. S. Measuring Dynamic Cell-Material Interactions and Remodeling during 3D Human Mesenchymal Stem Cell Migration in Hydrogels. *Proc. Natl. Acad. Sci. U. S. A.* 2015, 112 (29), E3757–E3764.
- (8) Chen, H. C.; Patel, V.; Wiek, J.; Rassam, S. M.; Kohner, E. M. Vessel Diameter Changes during the Cardiac Cycle. Eye 1994, 8 (Pt 1), 97–103.
- (9) Hao, H.; Sasongko, M. B.; Wong, T. Y.; Che Azemin, M. Z.; Aliahmad, B.; Hodgson, L.; Kawasaki, R.; Cheung, C. Y.; Wang, J. J.; Kumar, D. K. Does Retinal Vascular Geometry Vary with Cardiac Cycle? *Invest. Ophthalmol. Vis. Sci.* 2012, 53 (9), 5799– 5805
- (10) Weisel, J. W.; Litvinov, R. I. Fibrin Formation, Structure and Properties. *Subcell. Biochem.* **2017**, *82*, 405–456.
- (11) Seliktar, D. Designing Cell-Compatible Hydrogels for Biomedical Applications. *Science* **2012**, *336* (6085), 1124–1128.
- (12) Hoffman, A. S. Hydrogels for Biomedical Applications. *Adv. Drug Deliv. Rev.* **2012**, *64*, 18–23.
- (13) Tibbitt, M. W.; Anseth, K. S. Hydrogels as Extracellular Matrix Mimics for 3D Cell Culture. *Biotechnol. Bioeng.* 2009, 103 (4), 655–663.
- (14) Chen, J.; Peng, Q.; Peng, X.; Han, L.; Wang, X.; Wang, J.; Zeng, H. Recent Advances in Mechano-Responsive Hydrogels for Biomedical Applications. ACS Appl. Polym. Mater. 2020, 2 (3), 1092–1107.
- (15) Lim, H. L.; Hwang, Y.; Kar, M.; Varghese, S. Smart Hydrogels as Functional Biomimetic Systems. *Biomater Sci* **2014**, 2 (5), 603–618
- (16) Loebel, C.; Rodell, C. B.; Chen, M. H.; Burdick, J. A. Shear-Thinning and Self-Healing Hydrogels as Injectable Therapeutics and for 3D-Printing. *Nat. Protoc.* 2017, 12 (8), 1521–1541.
- (17) Highley, C. B.; Rodell, C. B.; Burdick, J. A. Direct 3D Printing of Shear-Thinning Hydrogels into Self-Healing Hydrogels. Adv. Mater. 2015, 27 (34), 5075–5079.
- (18) Xiang, Y.; Xian, S.; Ollier, R. C.; Yu, S.; Su, B.; Pramudya, I.; Webber, M. J. Diboronate Crosslinking: Introducing Glucose Specificity in Glucose-Responsive Dynamic-Covalent Networks. *J. Control. Release* **2022**, 348, 601–611.
- (19) Yu, S.; Ye, Z.; Roy, R.; Sonani, R. R.; Pramudya, I.; Xian, S.; Xiang, Y.; Liu, G.; Flores, B.; Nativ-Roth, E.; Bitton, R.; Egelman, E. H.; Webber, M. J. Glucose-Triggered Gelation of Supramolecular Peptide Nanocoils with Glucose-Binding Motifs. Adv. Mater. 2023, 36, e2311498.
- (20) Rodell, C. B.; Kaminski, A. L.; Burdick, J. A. Rational Design of Network Properties in Guest-Host Assembled and Shear-Thinning Hyaluronic Acid Hydrogels. *Biomacromolecules* 2013, 14 (11), 4125–4134.
- (21) Guvendiren, M.; Lu, H. D.; Burdick, J. A. Shear-Thinning Hydrogels for Biomedical Applications. *Soft Matter* **2011**, *8* (2), 260–272.
- (22) Shi, L.; Ding, P.; Wang, Y.; Zhang, Y.; Ossipov, D.; Hilborn, J.

- Self-Healing Polymeric Hydrogel Formed by Metal-Ligand Coordination Assembly: Design, Fabrication, and Biomedical Applications. *Macromol. Rapid Commun.* **2019**, 40 (7), e1800837.
- (23) Uman, S.; Dhand, A.; Burdick, J. A. Recent Advances in Shearthinning and Self-healing Hydrogels for Biomedical Applications. J. Appl. Polym. Sci. 2020, 137 (25), 48668.
- (24) Cui, J.; Xu, R.; Dong, W.; Kaneko, T.; Chen, M.; Shi, D. Skin-Inspired Patterned Hydrogel with Strain-Stiffening Capability for Strain Sensors. ACS Appl. Mater. Interfaces 2023, 15 (41), 48736–48743.
- (25) Cui, J.; Chen, J.; Ni, Z.; Dong, W.; Chen, M.; Shi, D. High-Sensitivity Flexible Sensor Based on Biomimetic Strain-Stiffening Hydrogel. ACS Appl. Mater. Interfaces 2022, 14 (41), 47148–47156.
- (26) Lin, S.; Liu, J.; Liu, X.; Zhao, X. Muscle-like Fatigue-Resistant Hydrogels by Mechanical Training. *Proc. Natl. Acad. Sci. U. S. A.* **2019**, *116* (21), 10244–10249.
- (27) Wang, Z.; Lü, S.; Liu, Y.; Li, T.; Yan, J.; Bai, X.; Ni, B.; Yang, J.; Liu, M. Noncovalent Muscle-Inspired Hydrogel with Rapid Recovery and Antifatigue Property under Cyclic Stress. *ACS Appl. Mater. Interfaces* **2019**, *11* (34), 31393–31401.
- (28) Luo, J.; Li, S.; Xu, J.; Chai, M.; Gao, L.; Yang, C.; Shi, X. Biomimetic Strain-stiffening Hydrogel with Crimped Structure. *Adv. Funct. Mater.* **2021**, *31* (43), 2104139.
- (29) Erk, K. A.; Henderson, K. J.; Shull, K. R. Strain Stiffening in Synthetic and Biopolymer Networks. *Biomacromolecules* 2010, 11 (5), 1358–1363.
- (30) Storm, C.; Pastore, J. J.; MacKintosh, F. C.; Lubensky, T. C.; Janmey, P. A. Nonlinear Elasticity in Biological Gels. *Nature* 2005, 435 (7039), 191–194.
- (31) Jaspers, M.; Dennison, M.; Mabesoone, M. F. J.; MacKintosh, F. C.; Rowan, A. E.; Kouwer, P. H. J. Ultra-Responsive Soft Matter from Strain-Stiffening Hydrogels. *Nat. Commun.* 2014, 5, 5808.
- (32) Ollier, R. C.; Xiang, Y.; Yacovelli, A. M.; Webber, M. J. Biomimetic Strain-Stiffening in Fully Synthetic Dynamic-Covalent Hydrogel Networks. Chem. Sci. 2023, 14 (18), 4796– 4805.
- (33) Wang, W.; Xiang, L.; Diaz-Dussan, D.; Zhang, J.; Yang, W.; Gong, L.; Chen, J.; Narain, R.; Zeng, H. Dynamic Flexible Hydrogel Network with Biological Tissue-like Self-Protective Functions. *Chem. Mater.* **2020**, *32* (24), 10545–10555.
- (34) Yan, B.; Huang, J.; Han, L.; Gong, L.; Li, L.; Israelachvili, J. N.; Zeng, H. Duplicating Dynamic Strain-Stiffening Behavior and Nanomechanics of Biological Tissues in a Synthetic Self-Healing Flexible Network Hydrogel. ACS Nano 2017, 11 (11), 11074– 11081
- (35) Liu, Y.; Lin, S.-H.; Chuang, W.-T.; Dai, N.-T.; Hsu, S.-H. Biomimetic Strain-Stiffening in Chitosan Self-Healing Hydrogels. ACS Appl. Mater. Interfaces 2022, 14 (14), 16032– 16046.
- (36) Chen, W.; Kumari, J.; Yuan, H.; Yang, F.; Kouwer, P. H. J. Toward Tissue-Like Material Properties: Inducing In Situ Adaptive Behavior in Fibrous Hydrogels. Adv. Mater. 2022, 34 (37), e2202057.
- (37) Marco-Dufort, B.; Iten, R.; Tibbitt, M. W. Linking Molecular Behavior to Macroscopic Properties in Ideal Dynamic Covalent Networks. J. Am. Chem. Soc. 2020, 142 (36), 15371–15385.
- (38) Bertula, K.; Martikainen, L.; Munne, P.; Hietala, S.; Klefström, J.; Ikkala, O.; Nonappa. Strain-Stiffening of Agarose Gels. ACS Macro Lett. 2019, 8 (6), 670–675.
- (39) Fernández-Castaño Romera, M.; Lou, X.; Schill, J.; Ter Huurne, G.; Fransen, P.-P. K. H.; Voets, I. K.; Storm, C.; Sijbesma, R. P. Strain-Stiffening in Dynamic Supramolecular Fiber Networks. J. Am. Chem. Soc. 2018, 140 (50), 17547–17555.

- (40) Barbucci, R.; Magnani, A.; Consumi, M. Swelling Behavior of Carboxymethylcellulose Hydrogels in Relation to Cross-Linking, pH, and Charge Density. *Macromolecules* 2000, 33 (20), 7475–7480.
- (41) Huang, Z.; Delparastan, P.; Burch, P.; Cheng, J.; Cao, Y.; Messersmith, P. B. Injectable Dynamic Covalent Hydrogels of Boronic Acid Polymers Cross-Linked by Bioactive Plant-Derived Polyphenols. *Biomater Sci* 2018, 6 (9), 2487–2495.
- (42) Chen, C.; Yang, H.; Yang, X.; Ma, Q. Tannic Acid: A Crosslinker Leading to Versatile Functional Polymeric Networks: A Review. RSC Adv. 2022, 12 (13), 7689–7711.
- (43) Brooks, W. L. A.; Sumerlin, B. S. Synthesis and Applications of Boronic Acid-Containing Polymers: From Materials to Medicine. Chem. Rev. 2016, 116 (3), 1375–1397.
- (44) Yesilyurt, V.; Webber, M. J.; Appel, E. A.; Godwin, C.; Langer, R.; Anderson, D. G. Injectable Self-Healing Glucose-Responsive Hydrogels with pH-Regulated Mechanical Properties. Adv. Mater. 2016, 28 (1), 86–91.
- (45) Krezanoski, J. Z. Tannic Acid: Chemistry, Analysis, and Toxicology. An Episode in the Pharmaceutics of Radiology. *Radiology* **1966**, *87* (4), 655–657.
- (46) Matsumoto, A.; Ishii, T.; Nishida, J.; Matsumoto, H.; Kataoka, K.; Miyahara, Y. A Synthetic Approach toward a Self-Regulated Insulin Delivery System. *Angew. Chem. Weinheim Bergstr. Ger.* 2012, 124 (9), 2166–2170.
- (47) Springsteen, G.; Wang, B. A Detailed Examination of Boronic Acid-diol Complexation. *Tetrahedron* 2002, 58 (26), 5291–5300.
- (48) Brooks, W. L. A.; Deng, C. C.; Sumerlin, B. S. Structure-Reactivity Relationships in Boronic Acid-Diol Complexation. ACS Omega 2018, 3 (12), 17863–17870.
- (49) Maier, G. P.; Bernt, C. M.; Butler, A. Catechol Oxidation: Considerations in the Design of Wet Adhesive Materials. *Biomater Sci* 2018, 6 (2), 332–339.
- (50) Boral, S.; Saxena, A.; Bohidar, H. B. Syneresis in Agar Hydrogels. Int. J. Biol. Macromol. 2010, 46 (2), 232–236.
- (51) Le, X. T.; Rioux, L.-E.; Turgeon, S. L. Formation and Functional Properties of Protein-Polysaccharide Electrostatic Hydrogels in Comparison to Protein or Polysaccharide Hydrogels. *Adv. Colloid Interface Sci.* 2017, 239, 127–135.
- (52) Ako, K. Influence of Elasticity on the Syneresis Properties of κ-Carrageenan Gels. *Carbohydr. Polym.* **2015**, *115*, 408–414.
- (53) Pezron, E.; Leibler, L.; Ricard, A.; Audebert, R. Reversible Gel Formation Induced by Ion Complexation. 2. Phase Diagrams. *Macromolecules* 1988, 21 (4), 1126–1131.
- (54) Pezron, E.; Ricard, A.; Leibler, L. Rheology of Galactomannanborax Gels. J. Polym. Sci. B Polym. Phys. 1990, 28 (13), 2445–2461.
- (55) Lopez, C. G.; Rogers, S. E.; Colby, R. H.; Graham, P.; Cabral, J. T. Structure of Sodium Carboxymethyl Cellulose Aqueous Solutions: A SANS and Rheology Study. J. Polym. Sci. B Polym. Phys. 2015, 53 (7), 492–501.
- (56) Huang, G.; Zhang, H.; Liu, Y.; Chang, H.; Zhang, H.; Song, H.; Xu, D.; Shi, T. Strain Hardening Behavior of Poly(vinyl alcohol)/Borate Hydrogels. *Macromolecules* 2017, 50 (5), 2124– 2135.
- (57) Yu, A. C.; Lian, H.; Kong, X.; Lopez Hernandez, H.; Qin, J.; Appel, E. A. Physical Networks from Entropy-Driven Non-Covalent Interactions. *Nat. Commun.* 2021, 12 (1), 746.
- (58) Xian, S.; Webber, M. J. Temperature-Responsive Supramolecular Hydrogels. J. Mater. Chem. B Mater. Biol. Med. 2020, 8 (40), 9197–9211.
- (59) Parada, G. A.; Zhao, X. Ideal Reversible Polymer Networks. Soft Matter 2018, 14 (25), 5186–5196.
- (60) Lee, H.; Dellatore, S. M.; Miller, W. M.; Messersmith, P. B. Mussel-Inspired Surface Chemistry for Multifunctional

- Coatings. Science 2007, 318 (5849), 426-430.
- (61) Dai, Q.; Geng, H.; Yu, Q.; Hao, J.; Cui, J. Polyphenol-Based Particles for Theranostics. *Theranostics* 2019, 9 (11), 3170–3190.
- (62) Ye, D.; Cheng, Q.; Zhang, Q.; Wang, Y.; Chang, C.; Li, L.; Peng, H.; Zhang, L. Deformation Drives Alignment of Nanofibers in Framework for Inducing Anisotropic Cellulose Hydrogels with High Toughness. ACS Appl. Mater. Interfaces 2017, 9 (49), 43154–43162.
- (63) Oćwieja, M.; Adamczyk, Z.; Morga, M. Adsorption of Tannic Acid on Polyelectrolyte Monolayers Determined in Situ by Streaming Potential Measurements. J. Colloid Interface Sci. 2015, 438, 249–258.
- (64) Sigala, P. A.; Ruben, E. A.; Liu, C. W.; Piccoli, P. M. B.; Hohenstein, E. G.; Martínez, T. J.; Schultz, A. J.; Herschlag, D. Determination of Hydrogen Bond Structure in Water versus Aprotic Environments To Test the Relationship Between Length and Stability. J. Am. Chem. Soc. 2015, 137 (17), 5730–5740.
- (65) Herschlag, D.; Pinney, M. M. Hydrogen Bonds: Simple after All? *Biochemistry* **2018**, *57* (24), 3338–3352.
- (66) Tummala, G. K.; Joffre, T.; Rojas, R.; Persson, C.; Mihranyan, A. Strain-Induced Stiffening of Nanocellulose-Reinforced Poly(vinyl Alcohol) Hydrogels Mimicking Collagenous Soft Tissues. Soft Matter 2017, 13 (21), 3936–3945.
- (67) Zhu, S.; Wang, S.; Huang, Y.; Tang, Q.; Fu, T.; Su, R.; Fan, C.; Xia, S.; Lee, P. S.; Lin, Y. Bioinspired Structural Hydrogels with Highly Ordered Hierarchical Orientations by Flow-Induced Alignment of Nanofibrils. *Nat. Commun.* 2024, 15 (1), 118.
- (68) Webber, M. J.; Tibbitt, M. W. Dynamic and Reconfigurable Materials from Reversible Network Interactions. *Nature Reviews Materials* 2022, 7 (7), 541–556.
- (69) Liu, J.; He, X.; Zhang, J. Z. H.; Qi, L.-W. Hydrogen-Bond Structure Dynamics in Bulk Water: Insights from Ab Initio Simulations with Coupled Cluster Theory. *Chem. Sci.* 2018, 9 (8), 2065–2073.
- (70) Nam, S.; Hu, K. H.; Butte, M. J.; Chaudhuri, O. Strain-Enhanced Stress Relaxation Impacts Nonlinear Elasticity in Collagen Gels. Proc. Natl. Acad. Sci. U. S. A. 2016, 113 (20), 5492–5497.
- (71) Bell, G. I. Models for the Specific Adhesion of Cells to Cells. Science 1978, 200 (4342), 618–627.
- (72) Andersson Trojer, M.; Andersson, M.; Bergenholtz, J.; Gatenholm, P. Elastic Strain-Hardening and Shear-Thickening Exhibited by Thermoreversible Physical Hydrogels Based on Poly(alkylene Oxide)-Grafted Hyaluronic Acid or Carboxymethylcellulose. Phys. Chem. Chem. Phys. 2020, 22 (26), 14579–14590.
- (73) Crowell, A. D.; FitzSimons, T. M.; Anslyn, E. V.; Schultz, K. M.; Rosales, A. M. Shear Thickening Behavior in Injectable Tetra-PEG Hydrogels Cross-Linked via Dynamic Thia-Michael Addition Bonds. *Macromolecules* 2023, 56 (19), 7795–7807.
- (74) Lopez Hernandez, H.; Souza, J. W.; Appel, E. A. A Quantitative Description for Designing the Extrudability of Shear-Thinning Physical Hydrogels. *Macromol. Biosci.* 2021, 21 (2), e2000295.
- (75) de Paiva Narciso, N.; Navarro, R. S.; Gilchrist, A. E.; Trigo, M. L. M.; Aviles Rodriguez, G.; Heilshorn, S. C. Design Parameters for Injectable Biopolymeric Hydrogels with Dynamic Covalent Chemistry Crosslinks. *Adv. Healthc. Mater.* 2023, 12 (27), e2301265.
- (76) Nicodemus, R. A.; Ramasesha, K.; Roberts, S. T.; Tokmakoff, A. Hydrogen Bond Rearrangements in Water Probed with Temperature-Dependent 2D IR. J. Phys. Chem. Lett. 2010, 1 (7), 1068–1072.
- (77) Jaishankar, A.; Wee, M.; Matia-Merino, L.; Goh, K. K. T.; McKinley, G. H. Probing Hydrogen Bond Interactions in a Shear Thickening Polysaccharide Using Nonlinear Shear and

Extensional Rheology. *Carbohydr. Polym.* **2015**, *123*, 136–145. (78) Pujol, T.; du Roure, O.; Fermigier, M.; Heuvingh, J. Impact of Branching on the Elasticity of Actin Networks. $Proc.\ Natl.\ Acad.$

SYNOPSIS:

Strain-stiffening and other mechanoresponsive behaviors of carboxymethyl cellulose hydrogels containing both dynamic-covalent crosslinks and inter-chain hydrogen bonding were characterized.

